Quantum Chemistry Based Force Field for Simulations of Poly(vinylidene fluoride)

Oleksiy G. Byutner and Grant D. Smith*

Department of Materials Science and Engineering and Department of Chemical and Fuels Engineering, University of Utah, 122 S. Central Campus Drive, Room 304, Salt Lake City, Utah 84112; and Richard L. Jaffe NASA Ames Research Center, Moffett Field, California 94035

Received October 29, 1999; Revised Manuscript Received March 10, 2000

ABSTRACT: A classical potential function for simulations of poly(vinylidene fluoride) (PVDF) based upon quantum chemistry calculations on PVDF oligomers has been developed. Quantum chemistry analysis of the geometries and conformational energies of 1,1,1,3,3-pentafluorobutane (PFB), 1,1,1,3,3,5,5,5-octofluoropentane (OFP), 2,2,4,4-tetrafluoropentane (TFP), and 2,2,4,4,6,6-hexafluoroheptane (HFH) was undertaken. In addition, an ab initio investigation of the energies of CF_4-CF_4 and CH_4-CF_4 dimers was performed. The classical potential function accurately reproduces the molecular geometries and conformational energies of the PVDF oligomers as well as intermolecular interactions between CH_4 and CF_4. To validate the force field, molecular dynamics simulations of a PVDF melts have been carried out at several temperatures. Simulation results are in good agreement with extant experimental data for PVT properties for amorphous PVDF as well as for PVDF chain dimensions.

I. Introduction

Poly(vinylidene fluoride) (PVDF or PVF_2) is a partially fluorinated polymer that possesses numerous desirable properties.[1] It is used in a large variety of applications in both the crystalline and amorphous states.[2] There are many commercial fluoropolymers synthesized as a pure PVDF (Hylar, Kynar, and others) or as fluoroelastomers such as Viton, which is 78% VDF copolymerized with 22% hexafluoropropylene. While PVDF has been studied extensively over the past 3 decades, little is understood about the equilibrium and dynamic conformational properties of the polymer in the amorphous phase, or the extent to which condensed phase (intermolecular) interactions are important in determining the conformational properties of the polymer.

In this paper, we present a new quantum chemistry based potential for PVDF that accurately reproduces the conformational energetics of a set of PVDF model compounds. The details and results of the force field fitting procedure are presented section II of this paper. To validate the quantum chemistry based potential function, we have performed a series of molecular dynamics (MD) simulations of PVDF melts at atmospheric pressure and at temperatures varying from 10 to 310 °C. We have investigated the density of the PVDF melts and the dimensions of the molecules as a function of temperature. In section III we compare results of our simulations of PVDF with experiment.

II. Force Field Parametrization

Several atomistic potentials for PVDF, both nonpolarizable[3] and polarizable,[3−6] have been developed. These force fields were derived for simulations of PVDF crystalline polymorphs and consequently have been empirically adjusted in order to reproduce experimental crystal properties including vibrational (phonon) frequencies and unit cell dimensions. While these potentials do a reasonable job in reproducing select crystal properties, conformational energetics in these potentials were based upon limited quantum chemistry calculations on 1,1,1,3,3-pentafluorobutane (PFB).[3,4] Subsequently, higher-level quantum chemistry calculations have shown that these potentials yield an incorrect picture of conformational energetics in PVDF model compounds.[3] In this paper, we present an explicit atom force field specifically derived for simulations of amorphous PVDF, where an accurate representation of conformational energetics is much more important than in a "fixed" conformation crystal phase.

We have recently performed an extensive high-level quantum chemistry study[7] of the conformational properties of four PVDF oligomers: PFB, 1,1,1,3,3,5,5,5-octofluoropentane (OFP), 2,2,4,4-tetrafluoropentane (TFP), and 2,2,4,4,6,6-hexafluoroheptane (HFH). Information gleaned from this study has allowed us to parametrize valence potential functions for PVDF. In addition, we have determined partial atomic charges for PVDF oligomers and the VDF monomer unit from the ab initio wave functions. Additionally, improvements in nonbonded potential parameters for PVDF have been undertaken based upon ab initio calculations of the interaction energies between CH_4 and CF_4 molecules. Following the procedure we have previously applied to a number of polymers,[8−10] we have parametrized a potential function for PVDF that accurately reproduces molecular geometries and conformational energies for model compounds obtained from quantum chemistry calculations. The total potential energy $V(\mathbf{r})$ of an ensemble of atoms whose positions are described by the coordinate vector $\mathbf{r}$ is represented as

$$V(\mathbf{r}) = V_{EL}(\mathbf{r}) + V_{vdW}(\mathbf{r}) + V_S(\mathbf{r}) + V_B(\mathbf{r}) + V_T(\mathbf{r}) \quad (1)$$

The first two terms (electrostatic and van der Waals potentials) describe the interaction of atoms not directly bonded (either through a covalent bond or valence bend interaction). We use a simple two-bond representation of the electrostatic energy

$$V_{EL}(\mathbf{r}) = \sum_{i>j} \frac{q_i q_j}{\epsilon r_{ij}} \quad (2)$$

* To whom correspondence should be addressed at the University of Utah.

10.1021/ma9918295 CCC: $19.00
Published on Web 05/04/2000

where q_i is the partial atomic charge on atom i, ϵ is the dielectric constant (set to unity), and r_{ij} is the distance between atoms i and j. The sum is over all nonbonded pairs. Similarly, the van der Waals energy is given by

$$V_{\mathrm{vdW}}(\mathbf{r}) = \sum_{i>j} A_{ij} \exp(-B_{ij} r_{ij}) - \frac{C_{ij}}{r_{ij}^{6}} \qquad (3)$$

The valence (stretching, bending and torsional) interactions are given by

$$V_{\mathrm{S}}(\mathbf{r}) = \sum_{i,j} \frac{1}{2} K_{ij}^{\mathrm{S}} (r_{ij} - r_{ij}^{\mathrm{o}})^2 \qquad (4)$$

$$V_{\mathrm{B}}(\mathbf{r}) = \sum_{i,j,k} \frac{1}{2} K_{ijk}^{\mathrm{B}} (\theta_{ijk} - \theta_{ijk}^{\mathrm{o}})^2 \qquad (5)$$

$$V_{\mathrm{T}}(\mathbf{r}) = \sum_{i,j,k,l} \sum_{n} \frac{1}{2} K(n)_{ijkl}^{\mathrm{T}} [1 - \cos(n\phi_{ijkl})] \qquad (6)$$

where θ_{ijk} and ϕ_{ijkl} are the valence and torsional angle formed by bonded atoms i, j, k and i, j, k, and l, respectively. The sums are over all bonds, bends, and torsions.

Quantum Chemistry Calculations. A detailed description of the quantum chemistry calculations performed on the PVDF oligomers can be found in our previous work.[7] In all previous quantum chemistry calculations as well as those described here, the quantum chemistry package *Gaussian94/Gaussian98*[11] was employed. Briefly, for the PVDF oligomers, SCF geometry optimizations were performed for the low energy conformers and rotational energy barriers in PFB, OFP, TFP and HFH using a D95** basis set. Subsequent single-point energy calculations were performed at the MP2 level of electron correlation using a D95+** basis set. Details of the quantum chemistry calculations employed in investigating molecular clusters used to improve van der Waals parameters are provided below.

Partial Atomic Charges. Partial atomic charges for the PVDF oligomers were obtained by determining the set of charges that best reproduces the electrostatic potential for a grid of points surrounding a given molecule in the lowest energy conformation, while at the same time accurately reproducing the molecular dipole moment. The electrostatic potential and molecular dipole moments were obtained from the MP2/D95+** wave functions. The electrostatic grid extended from 1.8 Å for hydrogen atoms, from 2.5 Å for carbon atoms, and from 2.0 Å for fluorine atoms to 4.0 Å from each atom. For each molecule, the electrostatic potential was evaluated at approximately 15 000 points. During the fitting procedure, atoms were divided onto six different charge groups; (i) carbon atoms in the CH_2 group (labeled C_H), (ii) carbon atoms in the CF_2 group (labeled C_F), (iii) carbon atoms in CH_3 termination group (labeled C_{H_3}), (iv) carbon atoms in CF_3 termination group (labeled C_{F_3}), (v) all hydrogen atoms (labeled H), and (vi) all fluorine atoms (labeled F). Within each molecule, all atoms of a given charge type were constrained to have equal charge.

Charges for each oligomer were fitted separately and results are shown in Table 1. It can be seen that for TFP, PFB, and HFH charges for the same atoms and atomic groups are similar, while the charges for OFP show somewhat larger deviations from the mean value.

Table 1. Partial Atomic Charges for PVDF Model Compounds

atoms/groups	PFB	OFP	TFP	HFH	force field[a]
$-(CH_2)-$	−0.1723	−0.0862	−0.1975	−0.1900	−0.1588
$-(CF_2)-$	+0.1912	+0.0946	+0.1669	+0.1710	+0.1588
$-(CH_3)-$	−0.0719		−0.0681	−0.0665	−0.0794
$-(CF_3)-$	+0.0533	+0.0348			+0.0794
$-(CH_2-CF_2)-$	+0.0189	+0.0084	−0.0306	−0.0190	0.0000
H	+0.1952	+0.1866	+0.1804	+0.1605	+0.1807
F	−0.2075	−0.1878	−0.2562	−0.2550	−0.2266
C_H	−0.5627	−0.4594	−0.5583	−0.5110	−0.5202
C_F	+0.6062	+0.4702	+0.6793	+0.6810	+0.6120
C_{H_3}	−0.6575		−0.6093	−0.5480	−0.6215
C_{F_3}	+0.6758	+0.5982			+0.7592

[a] In actual MD simulations charges were increased by 10% over those tabulated here.

Table 2. Nonbonded Force Field Parameters for PVDF

	Buckingham exponential/6 parameters		
atomic pair	*A*	*B*	*C*
C−C[a]	14976.0	3.0900	640.80
H−H[a]	2649.6	3.7400	27.36
F−F[a]	135782.0	4.5461	106.12
F−F[b]	112498.0	4.5223	66.21
F−F[c]	54115.2	4.3750	112.75
F−F[d]	153044.1		220.75
C−H[a]	4320.0	3.4150	138.24
C−F[a]	45094.0	3.8181	260.77
H−F[a]	12300.0	4.1431	53.88
H−F[e]	18967.6	4.1431	53.88
H−F[b]	15751.9	4.1064	47.99
H−F[d]	13150.8		45.64

[a] Parameters used in the current force field. [b] Parameters from ref 3. [c] Parameters from ref 12. [d] Parameters from ref 19 used in Lennard−Jones potential: $V_{\mathrm{L.J.}} = A/r^{12} - C/r^6$. [e] Parameters obtained by combining rules[16] from H−H and F−F potentials.

With the constraints that the polymer repeat unit and PVDF oligomers remain charge neutral, averaging yielded the force field partial atomic charges given in Table 1.

Van der Waals Parameters. The van der Waals parameters for carbon and hydrogen atoms were previously determined by Boyd et al.[12] and have been used extensively by us.[10,13−15] These parameters are given in Table 2 for convenience. To determine F−F and F−C van der Waals parameters, ab initio electronic structure calculations were performed on a CF_4-CF_4 dimer. The intermolecular interaction energy was determined as a function of separation along the C_3 axis for the configuration shown in Figure 1. Calculations were performed at the MP2/6-311G** level and binding energies were corrected for basis set superposition error (BSSE). The binding energy as a function of separation was fit by adjusting the F−F van der Waals parameters (see eq 3), while using values for C−C interactions previously determined[12] and standard combining rules for C−F interactions.[16] It was found that the quantum chemistry binding energies could be accurately represented in this fashion. The resulting force field was employed in MD simulations of liquid perfluorocyclobutane (PFCB). Charges of $q_C = 0.4136$ and $q_F = -0.2068$ were used as obtained from quantum chemistry. Simulations of 134 PFCB molecules at 263 K using the methodology described below yielded a large positive pressure at experimental density. Since BSSE corrected MP2 calculations at the level of theory employed here are likely to underestimate dispersion interactions,[17] the F−F dispersion parameter (C_{ij} in eq 3) was scaled by a factor

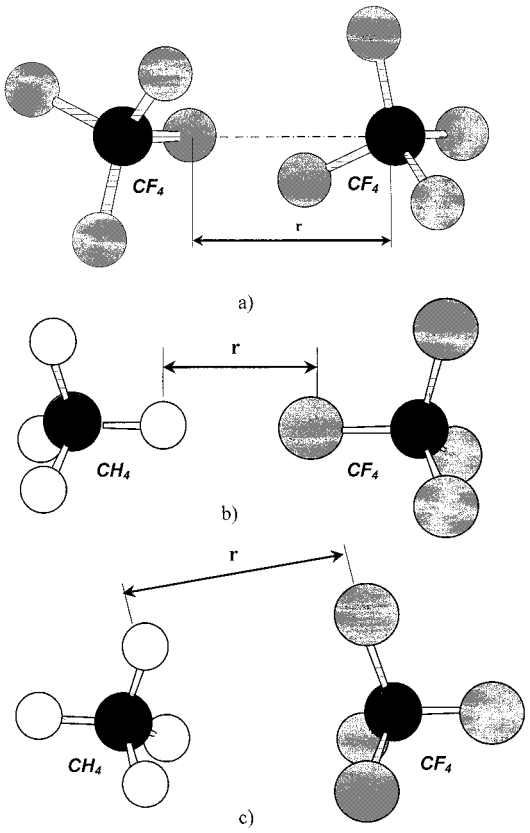

Figure 1. (a) Configuration of CF_4-CF_4 dimer in ab initio electronic structure calculations performed on intermolecular interaction energy as a function of separation along the C_3 axes. (b) Configuration of CH_4-CF_4 dimer in ab initio electronic structure calculations for path 1. (c) Same as part b for path 2.

of 1.4 in order to obtain near-zero pressure at experimental density for liquid PFCB. The resulting F−F parameters are given in Table 2. The F−F, C−F, and C−C nonbonded parameters given in Table 2 have been used subsequently in simulations of poly(tetrafluoroethylene) (PTFE) melts. These simulations yield PVT properties and the X-ray structure factor of PTFE melts as a function of temperature in good agreement with experiment.[18]

Using van der Waals parameters for H−F interactions obtained from standard combining rules[16] from the F−F and H−H parameters given in Table 2, we found poor agreement with experiment for the PVT properties of a PVDF melt. Therefore, in an attempt to improve agreement of PVT properties with experiment, we reparametrized the H−F van der Waals parameters. We performed quantum chemistry calculations on a CF_4-CH_4 dimer and computed the BSSE corrected intermolecular interaction energies as a function of separation for the configurations shown in Figure 1. Calculations were performed at the SCF/D95** level and are expected to accurately reproduce repulsive and electrostatic interactions between the molecules. Applying standard combining rules for A_{HF} and B_{HF} parameters and taking the other A_{ij} and B_{ij} parameters from Table 2 without dispersion ($C_{ij} = 0$), we obtained the CH_4-CF_4 interaction energy shown in Figure 2 (dashed lines). The molecular mechanics calculations yield a much more repulsive interaction than that obtained by ab initio calculations. This is consistent with the results obtained from preliminary MD simulations of PVDF melts using the same parameters (including dispersion), which

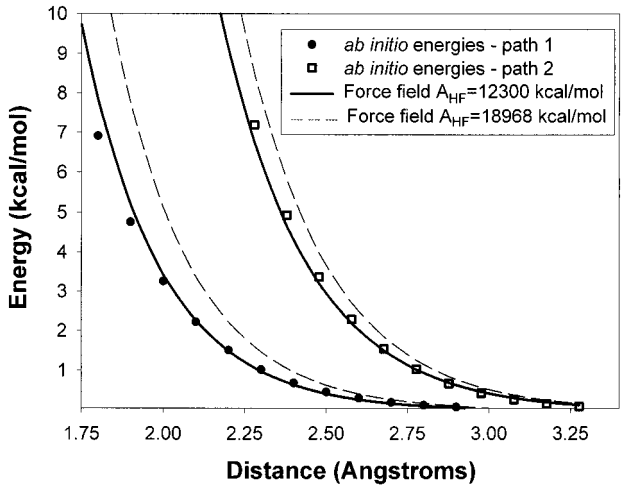

Figure 2. Energy vs separation for CF_4 and CH_4 model molecules calculated from quantum chemistry (BSSE-corrected) and fit. Key: black dots, path 1; open squares, path 2).

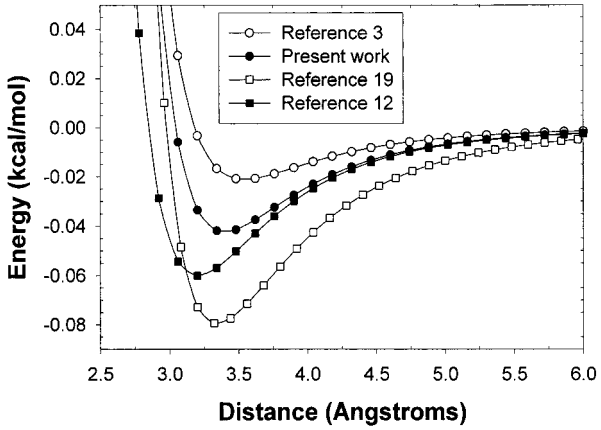

Figure 3. Nonbonded potential functions of fluorine−fluorine atomic pair.

yielded a density significantly lower than that observed experimentally. Thus, we adjusted parameter A_{HF} to yield a good representation of the $CH_4 - CF_4$ interaction energy obtained from quantum chemistry (also shown in Figure 2). The resulting parameter A_{HF}, with B_{HF} and C_{HF} derived from standard combining rules, are given in Table 2. Subsequent simulations of PVDF melts yielded PVT properties in excellent agreement with experiment (see section III of this paper).

A comparison of our F−F and H−F potentials with several potentials reported in the literature[3,12,19] is shown in Figures 3 and 4, respectively. Our F−F potential lies intermediate to the other potentials shown. Our F−F interaction is significantly more attractive than that of Karasawa et al.[3] used in previous simulations of PVDF. Similarly, our H−F potential lies intermediate to the other potentials shown, again being more attractive than that used in previous PVDF simulations.[3]

Empirical Charge Adjustment. Our quantum chemistry derived charges reproduce the electrostatic potential for isolated (gas phase) PVDF oligomers. Rutledge[5] has shown that for the β-phase of PVDF polarization plays an important role in intermolecular interactions increasing molecule dipoles up to 150% compared to the isolated molecule. To approximate induced dipole moments (polarization) resulting from intermolecular in-

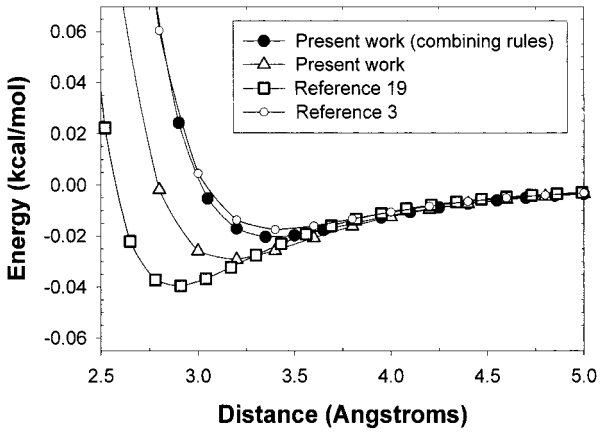

Figure 4. Nonbonded potential functions of hydrogen−fluorine atomic pair.

teractions, we calculated the gas-phase second virial coefficient for gaseous 1,1-difluoroethylene using the method described previously,[20] employing the nonbonded parameters given in Table 2. Reasonable agreement between the predicted gas-phase second virial coefficient and experiment was seen. However, agreement was improved when the dipole moment of the molecule was increased by 10% (through scaling of the quantum chemistry based partial atomic charges by a factor of 1.1), indicating that polarization effects have some influence on the strength of intermolecular interactions for this polar molecule, although not as large as in crystal phases. Simulations of PVDF melts were therefore performed using quantum chemistry based charges scaled by a factor of 1.1 (see Table 1). Increasing the charges was found to have only a small influence on PVT properties of the PVDF melt.

Valence Parameters. All equilibrium bond lengths and valence angles (eqs 4 and 5) were determined by fitting to the ab initio geometry of the lowest energy HFH conformation. Stretching force constants for all bonds as well as bending force constants for all bends except $F-C_F-F$ and $F-C_F-C_H$ were taken from ref 21. To determine force constants for the $F-C_F-F$ and $F-C_F-C_H$ bends, the energy of 2,2-difluoropropane was determined from MPZ/D95+* level quantum chemistry calculations as a function of the $F-C_F-F$ and $F-C_F-C_H$ valence angles, while other internal coordinates were left unchanged from their optimized values. The force constants for these bends were then adjusted to give the best fit to the energies of the "distorted" 2,2-difluoropropane as determined from quantum chemistry. All valence force field parameters are listed in Table 3.

Torsions. The properties of polymer melts are very sensitive to conformational populations as well as to conformational dynamics. Therefore, it is important to describe conformational energetics (conformational energies and rotational energy barriers) accurately. PVDF has one type of backbone dihedral, namely $C_H-C_F-C_H-C_F$, and three types of dihedrals involving pendent atoms, specifically $F-C_F-C_H-H$, $F-C_F-C_H-C_F$ and $H-C_H-C_F-C_H$. Here, the subscripts H and F indicate the carbon atoms of CH_2/CH_3 and CF_2/CF_3 atomic group, respectively.

Torsional parameters (eq 6) were adjusted to yield the best representation of the conformational energies and geometries of the low energy conformers of HFH. During the parametrization, greater weight was given to the

Table 3. Valence Force Field Parameters for PVDF Stretch Constants and Equilibrium Length for Bonds

bond type	K_S (kcal mol^{-1}Å^{-2})	R_0 (Å)
C_H[a]−H	655.2	1.0850
C_F[b]−F	998.6	1.3570
C_F−CH	617.8	1.5340
bend type	K_B (kcal mol^{-1}rad^{-2})	Θ_0 (deg)
F−C_F−F	240.0	105.27
F−C_F−C_H	180.0	107.74
C_H−C_F−C_H	160.6	118.24
H−C_H−H	77.0	109.27
H−C_H−C_F	85.8	108.45
C_F−C_H−C_F	160.6	118.24

[a] C_H specifies the carbon atom in CH_2 and CH_3 groups. [b] C_F specifies the carbon atom in CF_2 or CF_3 groups.

Table 4. Torsional Force Field Parameters for PVDF

	constant K_i					
torsion	1	2	3	4	5	6
$C_F-C_H-C_F-C_H$	0.790	1.440	−0.760	−0.410	0.850	−0.050
$F-C_F-C_H-C_F$	0.710	0.690	−0.760	0.280	0.290	−0.050

Table 5. Energies and Geometries of PFB Conformers

	conformer	Φ[a]	energy[a] (kcal/mol)	
1	g^+	**53.4** *54.0*	**0.00**	*0.00*
2	t_+	**175.3** *163.2*	**1.47**	*1.36*
3	g^+–t_+	**122.9** *122.9*[b]	**3.42**	*3.79*
4	*t* (saddle)	**180.0** *180.0*[b]	**1.49**	*1.47*
5	*cis*	**0.0** *0.0*[b]	**2.90**	*2.75*

[a] Bold font specifies values obtained from ab initio calculations; italic font specifies values obtained from molecular mechanic analysis. [b] Torsional angles were constrained.

energies and geometries of the lower energy conformers. We found that a good representation of the HFH conformational energies and geometries could be obtained by considering $C_H-C_F-C_H-C_F$ and $F-C_F-C_H-C_F$ dihedrals only. The parameters for the torsional potential (see eq 6) for our best fit are listed in Table 4.

The molecular mechanics geometries and energies are compared with SCF/D95** geometries and MP2/D95+** energies for PFB and TFP and with HFH molecules in Tables 5−7, respectively. Despite the fact that the parametrization was performed only for the HFH oligomer, good agreement for conformational energies and geometries is seen for all compounds.

Comparison with RIS Predictions. The number of possible low energy conformers of HFH is much greater than the limited set used in the force field parametrization. Using a quantum chemistry based rotational isomeric state (RIS) model for PVDF described in our previous paper,[7] we predicted a number of low energy conformers for HFH that were not included in force field parametrization. All HFH conformers with RIS energy of less than 2.0 kcal/mol, which are not listed in Table 7, are shown in Table 8. Quantum chemistry and molecular mechanics geometry optimizations were performed for these RIS predicted low energy conformations. In all cases (with one exception), both quantum chemistry and molecular mechanics calculations revealed these conformers to be unstable in HFH.

We believe the discrepancy between RIS predictions and molecular mechanics/quantum calculations for HFH

Table 6. Energies and Geometries of TFP Conformers

	conformer	Φ_1[a]	Φ_2[a]	energy[a] (kcal/mol)	
1	$g^+ g^+$	**58.7**	**58.7**	**0.00**	*0.00*
		56.9	*56.9*		
2	$g^+ t_-$	**50.3**	**167.9**	**0.91**	*1.20*
		51.6	*161.2*		
3	t_+t_+	**193.2**	**193.2**	**3.63**	*3.34*
		198.1	*198.1*		
4	$g^+g^-_-$	**50.8**	**−86.7**	**3.14**	*3.14*
		50.1	*−76.5*		
5	tcis	**180.0**	**0.0**	**3.83**	*4.20*
		180.0	*0.0*[b]		
6	tt	**180.0**	**180.0**	**3.93**	*3.82*
		180.0	*180.0*[b]		
7	tt_tg^+	**178.9**	**124.4**	**5.46**	*5.91*
		178.3	*124.4*[b]		
8	$g^+t\_g^+g^+$	**65.8**	**120.3**	**3.52**	*4.23*
		63.5	*120.3*[b]		

[a] Bold font specifies values obtained from ab initio calculations; italic font specifies values obtained from molecular mechanic analysis. [b] Torsional angles were constrained.

Table 7. Energies and Geometries of HFH Conformers

	conformer	Φ_1[a]	Φ_2[a]	Φ_3[a]	Φ_4[a]	energy[a] (kcal/mol)		RIS energy (kcal/mol)
1	$g^+g^+g^+g^+$	**65.3**	**65.1**	**65.1**	**65.3**	**0.00**	*0.00*	0.00
		60.7[b]	*62.6*	*62.6*	*60.7*			
2	$g^+g^+t_+g^-$	**53.9**	**62.0**	**188.4**	**−50.8**	**0.27**	*0.23*	0.35
		52.4	*57.4*	*198.1*	*−52.2*			
3	$g^+g^+t_-g^+$	**60.6**	**59.3**	**164.0**	**50.6**	**0.33**	*0.10*	0.25
		59.1	*56.7*	*160.0*	*51.8*			
4	$g^+g^+g^+t_+$	**64.0**	**61.2**	**66.6**	**187.2**	**0.48**	*0.72*	0.25
		59.2	*56.2*	*66.0*	*200.3*			
5	$t_+g^+g^+t_-$	**194.0**	**69.8**	**52.4**	**171.9**	**0.62**	*1.33*	0.85
		202.9	*67.3*	*51.7*	*163.8*			
6	$g^+t_-g^+t_-$	**51.3**	**165.5**	**51.1**	**168.0**	**0.81**	*0.91*	0.85
		52.1	*160.6*	*50.8*	*161.4*			
7	$g^+t_-t_-g^+$	**50.9**	**166.0**	**166.0**	**50.9**	**1.21**	*1.56*	1.30
		52.0	*160.3*	*160.3*	*52.0*			
8	$g^-t\_g^+t_-$	**−51.4**	**184.2**	**52.4**	**165.0**	**1.55**	*1.79*	0.95
		−51.7	*193.4*	*52.4*	*158.9*			
9	$g^+g^+t_+t_+$	**55.7**	**62.9**	**190.4**	**193.4**	**2.29**	*1.97*	2.70
		53.0	*57.3*	*197.4*	*197.1*			
10	$t_-t_-g^+t_-$	**165.9**	**163.7**	**50.4**	**167.2**	**2.93**	*2.70*	3.20
		161.6	*160.4*	*50.0*	*161.1*			
11	$g^-_-g^+t_-g^+$	**−86.0**	**50.8**	**164.2**	**50.6**	**3.09**	*2.84*	3.45
		−69.1	*56.6*	*155.8*	*52.2*			
12	$g^+t_-t_-t_-$	**50.0**	**165.5**	**164.0**	**165.8**	**3.52**	*3.62*	3.65
		51.4	*160.1*	*160.2*	*161.7*			
13	$t_-t_-t_-t_-$	**165.7**	**163.9**	**163.9**	**165.7**	**6.53**	*6.14*	6.00
		161.6	*160.2*	*160.2*	*161.6*			
14	*tttt*	**180.0**	**180.0**	**180.0**	**180.0**	**7.51**	*7.45*	
		180.0[b]	*180.0*[b]	*180.0*[b]	*180.0*[b]			

[a] Bold font specifies values obtained from ab initio calculations, italic font specifies values obtained from molecular mechanic analysis. [b] Torsional angles were constrained.

can be explained by the fact that the RIS model does not take into account the influence of the termination groups in the molecule. To test this supposition, we have analyzed the conformations of all seven carbon/four dihedral sequences analogous to HFH obtained from MD simulations of PVDF melt (VDF−C_{44}, see below). Results of this analysis are given in Table 8. It can be seen that all sequences predicted to be of low energy by the RIS model, but found to be unstable in both quantum chemistry and molecular mechanics calculations on HFH, do exist in the longer molecule and have appreciable populations.

III. Force Field Validation

Simulation Methodology. Molecular dynamics simulations of PVDF were carried out utilizing the force field

Table 8. Conformational Energies of $CH_3-CF_2-CH_2-CF_2-CH_2-CF_2-CH_3$ Molecule and Conformational Populations of Its Analog in Longer Chains

	conformer	energy[a] (kcal/mol)		RIS energy (kcal/mol)	population[b] (%)
1	$g^+g^+t_-g^-$	**N/S**[c]**→2**[d]	*N/S→2*	−0.10	5.56
2	$g^+g^+t_+g^+$	**N/S→3**	*N/S→3*	0.00	3.53
3	$g^-t_+g^+t_+$	**N/S→8**	*N/S→8*	0.15	2.08
4	$g^-t_-g^+t_-$	**N/S→8**	*N/S→8*	0.50	4.20
5	$g^+t_-g^+t_+$	**N/S→6**	*N/S→6*	0.50	3.68
6	$t_+g^+g^+t_+$	**N/S→5**	1.66	0.50	2.24
7	$g^+g^+g^+t_-$	**N/S→4**	*N/S→4*	0.60	4.39
8	$g^+t_+g^+t_-$	**N/S→6**	*N/S→6*	0.60	3.43
9	$g^-t_+g^+t_+$	**N/S→8**	*N/S→8*	0.60	1.23

[a] Bold font specifies values obtained from ab initio calculations; italic font specifies values obtained from molecular mechanic analysis. [b] Conformational populations of $-CH_2-CF_2-CH_2-CF_2-CH_2-CF_2-CH_2-$ sequences were collected from the melt simulations performed at 463 K. [c] Nonstable conformer, during the energy minimization process has converged to another stable conformer. [d] Conformer number from Table 7 to which the given unstable conformer converged.

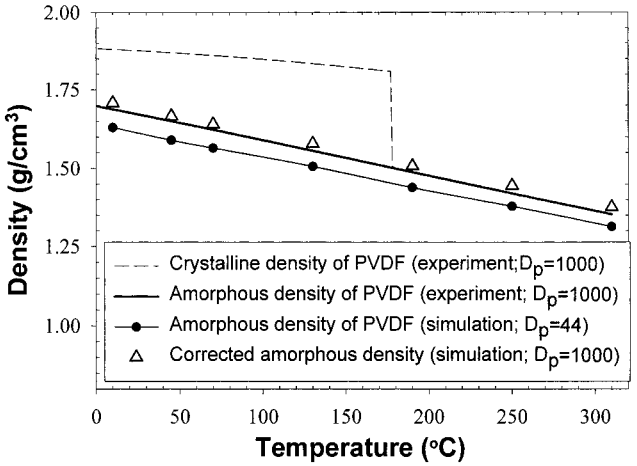

Figure 5. Density of amorphous and crystal PVDF vs temperature. Crystalline density is given for the α isomorphic state. Experimental samples (dashed line) had degree of polymerization of 1000, while simulated chains (black circles) consisted of 44 backbone carbons. Opened triangles show scaled densities of amorphous PVDF obtained from simulations to degree of polymerization of 1000. Scaling factor is 1.045.

described above. An ensemble of 40 molecules containing 21 repeat units each of the structure $CH_3-[CF_2-CH_2]_{21}-CF_3$ (VDF−C_{44}) was investigated. The initial system was generated by placing parallel all trans chains in a large periodic box, where the molecules were subject to random Brownian forces[22] until the end-to-end vectors of the chains had relaxed and their net orientation had disappeared. The density of the system was subsequently increased to the expected value. The system was then equilibrated using constant particle number, N, pressure, and temperature (NPT) dynamics at 523 K and 1 atm. After 500 ps the density of the system showed no further change with additional simulation time. Lower temperature systems were obtained by cooling this initial system at 1 atm under NPT conditions. After NPT volume equilibration had been established, the systems were switched to an NVT ensemble and prolonged trajectories were computed (approximately 2 ns for each temperature). Simulations were performed at 283, 343, 403, 463, 523, and 583 K. Simulations were performed using the constant tem-

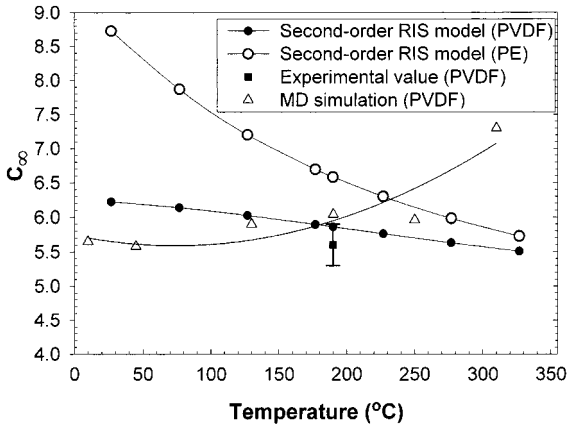

Figure 6. Characteristic ratio of PVDF chains calculated by RIS model (opened circles) and from liquid simulations (black triangles). Experimental value is given with an error-bar. For comparison also is shown characteristic ratio for PE calculated using the RIS model.

perature method of Nosé[23] in concert with the velocity−Verlet integrator[24] for NPT dynamics and with a multitime step integrator[24] for NVT dynamics. Bond lengths were constrained using the SHAKE algorithm[25] while other internal degrees of freedom (valence angle bends and torsions) remained flexible. Nonbonded dispersion interactions were truncated at 10.5 Å and long-range electrostatic interactions in the system were calculated employing the standard Ewald summation techniques[26] in all NPT and NVT ensembles.

PVT Behavior. We have compared the density of the PVDF melts as a function of temperature with experimental data[27] for amorphous PVDF (Kynar) for temperatures above and below the melting point (∼183 °C) at atmospheric pressure. It is not possible to make a direct comparison of these experimental densities with simulation results because the experimental samples had a degree of polymerization $D_p = 1000$, while in the simulation chains contained have $D_p = 44$, where D_p is the number of backbone carbon atoms. Since PVDF can be considered an alternating copolymer of polyethylene (PE) and poly(tetrafluoroethylene) (PTFE), we scale the simulation PVDF densities as

$$\rho_{\mathrm{PVDF}}^{\mathrm{scaled}}(1000) = \frac{\rho_{\mathrm{PE}}(1000) + \rho_{\mathrm{PTFE}}(1000)}{\rho_{\mathrm{PE}}(44) + \rho_{\mathrm{PTFE}}(44)} \rho_{\mathrm{PVDF}}^{\mathrm{sim}} \quad (12)$$

where subscripts indicate the polymer, the value in parentheses shows number of backbone carbon atoms, and the superscript sim indicates simulation results. For PE and PTFE density as a function of backbone carbons, we applied the following expressions[28]

$$\rho_{\mathrm{PE}}(D_p) = \left(1 - \frac{1.698}{D_p}\right)\rho_{\mathrm{PE}}^{\infty} \quad (13)$$

$$\rho_{\mathrm{PTFE}}(D_p) = \left(1 - \frac{2.275}{D_p}\right)\rho_{\mathrm{PTFE}}^{\infty} \quad (14)$$

where ρ^∞ is amorphous density of the polymer with infinite molecular weight at 180 °C ($\rho_{\mathrm{PE}}^{\infty}$ and $\rho_{\mathrm{PTFE}}^{\infty}$). Figure 5 shows the density of amorphous PVDF as a function of temperature obtained from simulation and scaled values for $D_p = 1000$. Experimental densities of amorphous and crystalline PVDF are also shown in Figure 5. The scaled simulation density is in good agreement with experiment over the entire temperature range.

Chain Dimensions. Chain dimensions of PVDF are represented by the characteristic ratio

$$C_\infty = \lim_{n\to\infty} \frac{\langle r^2 \rangle}{nl^2} \quad (16)$$

where $\langle r^2 \rangle$ is the mean-square end-to-end distance, n is the number of backbone bonds, and l is the bond length. The Θ temperature for the PVDF in benzophenone as reported by Welch[29] is 190 °C. The reported characteristic ratio for PVDF molecules under the theta-conditions is $C_\infty = 5.6 \pm 0.3$.[29] As our simulations have been performed on relatively short VDF−C_{44} chains, we estimated C_∞ by calculating the characteristic ratio as a function of $1/n$ using the relationship

$$C\left(\frac{1}{n}\right) = \frac{1}{N_C}\sum_{j=1}^{Nc}\frac{1}{44-n}\sum_{i=1}^{44-n}\frac{(\vec{r}_i^{\,j} - \vec{r}_{i+n}^{\,j})}{nl^2} \quad (17)$$

and then linearly extrapolating its value to $1/n \to 0$. Here n runs from $n = 1$ to 43 (number of backbone bonds), $\vec{r}_i^{\,j}$ and $\vec{r}_{i+n}^{\,j}$ are positions of the ith and $(i + n)$th carbon atom respectively in the jth chain, and N_C is the total number of chains in the system. The characteristic ratio as a function of temperature for the various models is shown in Figure 6. At 190 °C molecular dynamics simulation yields $C_\infty = 5.96$, while the second-order RIS model[7] yields $C_\infty = 5.86$. Both values are in good agreement with experiment.

The melt chains yield a C_∞ quite similar to the unperturbed chains (RIS model) at At 190 °C. However, unlike RIS chains, the melt chains show a positive temperature dependence for the characteristic ratio. The difference in the temperature dependence of chain dimensions for PVDF between the melt and RIS predictions must be due to intermolecular interactions. Hence, it is apparent that condensed phase effects are important in determining the conformations of melt PVDF chains as well as the preferred conformations in the crystalline polymorphs, as discussed previously.[7] The conformational statistics of PVDF melts, together with conformational and chain dynamics, will be considered in detail in future publications.

Acknowledgment. This research is funded in part by the University of Utah Center for the Simulation of Accidental Fires and Explosions (C-SAFE), funded by the Department of Energy, Lawrence Livermore National Laboratory, under Subcontract B341493.

References and Notes

(1) For a comprehensive review of the properties of PVDF, see: Lovinger, A. J. Poly(vinylidene fluoride). in *Developments in Crystalline Polymers-1*; Bassett, D. C., Ed.; Applied Science: Oxford, U.K., 1982; pp 195−273.
(2) Wang, T. T., Herbert, J. M., Glass, A. M., Eds: *The Application of Ferroelectric Polymers*; Chapman and Hall: New York, 1987.
(3) Karasawa, N.; Goddard, W. A., III. *Macromolecules* **1992**, *25*, 7268.
(4) Karasawa, N.; Goddard, W. A., III. *Macromolecules* **1995**, *28*, 6765.
(5) Carbeck, J. D.; Rutledge, G. C. *J. Comput.-Aided Mater. Des.* **1993**, *1*, 97.
(6) Carbeck, J. D.; Lacks, D. J.; Rutledge, G. C. *J. Chem. Phys.* **1995**, *103*, 10347.

(7) Byutner, O.; Smith, G. D. *Macromolecules* **1999**, *32*, 8376.
(8) Smith, G. D.; Yoon, D. Y. *J. Chem. Phys.* **1994**, *100*, 649.
(9) Jaffe, R. L.; Smith, G. D.; Yoon, D. Y. *J. Phys. Chem.* **1993**, *97*, 12752.
(10) Bedrov, D.; Pekny, M.; Smith, . D. *J. Phys. Chem.* **1998**, *102*, 996.
(11) Frisch, M. J.; Trucks, G. W.; Schlegel, H. B.; Scuseria, G. E.; Robb, M. A.; Cheeseman, J. R.; Zakrzewski, V. G.; Montgomery, J. A., Jr.; Stratmann, R. E.; Burant, J. C.; Dapprich, S.; Millam, J. M.; Daniels, A. D.; Kudin, K. N.; Strain, M. C.; Farkas, O.; Tomasi, J.; Barone, V.; Cossi, M.; Cammi, R.; Mennucci, B.; Pomelli, C.; Adamo, C.; Clifford, S.; Ochterski, J.; Petersson, G. A.; Ayala, J. Y.; Cui, Q.; Morokuma, K.; Malick, D. K.; Rabuck, A. D.; Raghavachari, K.; Foresman, J. B.; Cioslowski, J.; Ortiz, J. V.; Stefanov, B. B.; Liu, G.; Liashenko, A.; Piskorz, P.; Komaromi, I.; Gomperts, R.; Martin, R. L.; Fox, D. J.; Keith, T.; Al-Laham, M. A.; Peng, C. Y.; Nanayakkara, A.; Gonzalez, C.; Challacombe, M.; Gill, P. M. W.; Johnson, B.; Chen, A.; Wong, M. W.; Andres, J. L.; Gonzalez, C.; Head-Gordon, M.; Replogle, E. S.; Pople, J. A. *Gaussian 98, Revision A.1* Gaussian, Inc.: Pittsburgh, PA, 1998.
(12) Boyd, R. H.; Kesner, L. *J. Chem. Phys.* **1980**, *72*, 2179.
(13) Smith, G. D.; Jaffe, R. L.; Yoon, D. Y. *Macromolecules* **1993**, *26*, 298.
(14) Smith, G. D.; Borodin, O.; Pekny, M.; Annis, B.; Londono, D.; Jaffe, R. L. *Spectrochim. Acta* **1997**, *A53*, 1273.
(15) Smith, G. D.; Bharadwaj, R. K.; Bedrov, D.; Ayyagari, C. *J. Phys. Chem. B* **1999**, *103*, 705.
(16) Standard combining rules for exponential-6 potential: $A_{ij} = (A_{ii}A_{jj})^{1/2}$; $B_{ij} = (B_{ii} + B_{jj})/2$; $C_{ij} = (C_{ii}C_{jj})^{1/2}$.
(17) Williams, D. E. *Acta Crystallogr.* **1980**, *A36*, 715.
(18) Habenschuss, Anton. Private communications.
(19) Jedlovszky, P.; Mezei, M. *J. Chem. Phys.* **1999**, *110*, 2991.
(20) Smith, G. D.; Jaffe, R. L.; Yoon, D. Y. *J. Phys. Chem.* **1993**, *97*, 12752.
(21) Boyd, R. H.; Sanwal, S. N.; Shary-Tehrany, S.; McNally, D. *J. Phys. Chem.* **1971**, *75*, 1264.
(22) van Gunsteren, W. F.; Berendsen, H. J. C. *Mol. Phys.* **1982**, *45*, 637.
(23) Nosé, S. *J. Chem. Phys.* **1984**, *81*, 512.
(24) Martyna, G. J.; Tuckerman, M. E.; Tobias, D. J.; Klein, M. L. *Mol. Phys.* **1996**, *87*, 1117.
(25) Ryckaert, J. P.; Ciccotti, G.; Berendsen, H. J. C. *J. Chem. Phys.* **1993**, *98*, 10037.
(26) Allen, M. P.; Tildesley, D. J. *Computer Simulations of Liquids*; Clarendon Press: Oxford, U.K., 1987.
(27) Nakagawa, K.; Ishida, Y. *Kolloid-Z. Z. Polym.* **1973**, *251*, 103.
(28) Dee, G. T.; Sauer, B. B.; Haley, B. J. *Macromolecules* **1994**, *27*, 6106.
(29) Welch, G. J. *Polymer* **1974**, *15*, 429.

MA9918295